Time-domain reflectance diffuse optical tomography for imaging breast cancer

Time-domain reflectance diffuse optical tomography for imaging breast cancer

Kenji Yoshimoto*[a], Hiroko Wada[a], Nobuko Yoshizawa[b], Hiroyuki Ogura[c], Etsuko Ohmae[a], Hiroaki Suzuki[a], Shu Homma[a], Tetsuya Mimura[a], Norihiro Suzuki[a], Yuko Asano[c], Satoshi Goshima[b] and Yukio Ueda[a]

[a]Central Research Laboratory, Hamamatsu Photonics K.K., 5000, Hirakuchi, Hamakita-ku, Hamamatsu City, Shizuoka, 434-8601 Japan; [b]Department of Diagnostic Radiology and Nuclear Medicine, Hamamatsu University School of Medicine, 1-20-1 Handayama, Higashi-ku, Hamamatsu City, Shizuoka, 431-3192, Japan; [c]Department of Breast Surgery, Hamamatsu University School of Medicine, 1-20-1 Handayama, Higashi-ku, Hamamatsu City, Shizuoka, 431-3192, Japan

ABSTRACT

We report a time-domain reflectance diffuse optical tomography (TD-RDOT) system for providing three-dimensional images of hemoglobin concentration, tissue oxygen saturation, water and lipid contents of breast cancer from reflectance measurements. A scan area of 5 × 5 grid points with a 10-mm spacing is marked on the breast surface so that the tumor is just below the center of the area. The breast scan is performed by measuring the temporal profiles of six wavelengths at each grid point using a time-domain diffuse optical spectroscopy (TD-DOS) system and a hand-held probe. The TD-DOS system that we developed is capable of measuring water and lipid contents and hemoglobin concentration. The hand-held probe is designed to measure the breast in reflectance mode with a source-to-detector separation of 20 mm. The three-dimensional distributions of the tissue parameters are restored using an iterative image reconstruction method. As a preliminary clinical demonstration, a breast cancer patient with a tumor size of approximately 20 mm was examined with the TD-RDOT. The reconstructed images show that the breast cancer had high hemoglobin concentration and water content, and low tissue oxygen saturation and lipid content. The results indicate that the TD-RDOT system has the potential to provide diagnostically relevant information on the tissue characteristics of the tumor at the bedside.

Keywords: Diffuse optical tomography, time-domain, hand-held probe, breast cancer, chemotherapy monitoring

INTRODUCTION

Diffuse optical spectroscopy (DOS) is a technique for noninvasively measuring absolute values or changes in the concentrations of chromophores such as oxyhemoglobin (O_2Hb), deoxyhemoglobin (HHb), water, and lipid, in various human tissues. The optical absorption and scattering characteristics of tissue are quantified by DOS at several wavelengths in the near-infrared region (650–1000 nm), and the tissue parameters are then obtained from the absorption coefficients. DOS has a large variety of medical applications, including imaging and spectroscopy of breast cancer, monitoring of muscle diseases, and functional imaging of the brain. Many spectroscopy-based studies have been conducted within the field of breast cancer imaging, with the aims of classifying breast cancer, predicting breast cancer risk, and monitoring the responses to neoadjuvant chemotherapy[1]. Time-domain diffuse optical spectroscopy (TD-DOS) was used to classify breast lesions on the basis of their optically-quantified tissue composition, and it was demonstrated that collagen was the most important factor[2]. Diffuse optical spectroscopic imaging (DOSI) and diffuse correlation spectroscopy (DCS) can be combined to enhance breast tumor characterization, allowing images of tissue composition and blood flow index to be obtained[3]. Biomarkers of breast cancer risk have been investigated using maximum intensity projections generated by a diffuse optical tomography imaging system, and showed a correlation between mammographic breast density and O_2Hb[4]. Parameters derived from DOSI, such as the tissue optical index (TOI)[5], z-score normalization of the tissue oxygen saturation (StO_2)[6], and change in O_2Hb[7], have been studied as predictors of pathologic complete response to neoadjuvant chemotherapy for the treatment of breast cancer.

*k-yoshimoto@crl.hpk.co.jp; phone +81 53 586 7111; fax +81 53 586 6180

Reflectance-mode diffuse optical tomography (DOT) using a hand-held probe was also studied to obtain three-dimensional images of representative features of breast cancer and to contribute to the monitoring of treatment responses. Ultrasound (US) guided DOT with an imaging algorithm using co-registered US images was developed to locate and characterize breast lesions[8], and multispectral time-domain DOT in reflectance mode suitable for breast cancer imaging was investigated through the measurement of phantoms containing small inclusions[9]. We previously developed a time-domain reflectance diffuse optical tomography (TD-RDOT) system that provides three-dimensional distributions of total hemoglobin concentration (tHb), StO_2, and absorption and reduced scattering coefficients[10]. This twelve-channel TD-RDOT system scanned the breast automatically with light sources of three wavelengths (760, 800, and 830 nm), and was not capable of measuring water and lipid contents, as well as being somewhat large for bedside use.

In this paper, we present a TD-RDOT system designed to provide three-dimensional images of tissue parameters and monitor responses to breast cancer chemotherapy at the bedside. A manual scan using a single-channel TD-DOS system and a hand-held probe is employed to downsize the system. The TD-DOS system with a six-wavelength light source can quantify water and lipid contents in addition to tHb and StO_2. The TD-DOS system and hand-held probe are described as the key components of the TD-RDOT system. We also report a TD-RDOT scan of the breast and an iterative image reconstruction method. A preliminary clinical measurement was carried out to investigate the performance of our TD-RDOT system.

MATERIALS AND METHODS

Instrumentation

The TD-RDOT system consists of a single-channel TD-DOS system, a hand-held probe, and a workstation. Figure 1 presents a block diagram of the main components of the TD-DOS system. The breast is irradiated with a six-wavelength pulsed laser (761, 802, 838, 908, 936, and 976 nm) through a 1-mm diameter source optical fiber bundle with a numerical aperture (NA) of 0.29. The light that propagated in the tissue is collected by a 3-mm diameter detector optical fiber bundle with an NA of 0.29 and is guided to two photomultiplier tubes (GaAs PMT for 761, 802, and 838 nm; InGaAs PMT for 908, 936, and 976 nm) after passing through variable optical attenuators. The temporal profile is acquired by processing the detected light with a time-correlated single photon counting (TCSPC) circuit consisting of a constant fraction discriminator (CFD), a time-to-amplitude converter (TAC), an analog-to-digital (A/D) converter, and a histogram memory. The performance of the TD-DOS was demonstrated in our previous studies[11–13].

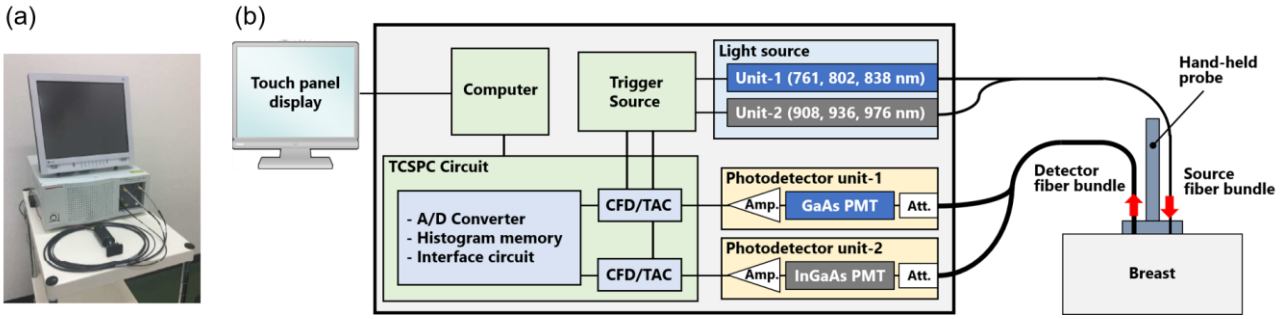

Figure 1. Time-domain diffuse optical spectroscopy system: (a) appearance and (b) block diagram.

TD-RDOT scan of the breast

The scan areas for a typical breast measurement are indicated in Fig. 2(a). The 5 × 5 grid points with a 10-mm spacing are marked on the breast surface so that the tumor is just below the center of the scan area. Grid points covering the same area are also marked in symmetrical positions on the contralateral normal breast. The breast scan is performed by measuring the temporal profiles of six wavelengths at each grid point using a hand-held probe designed to measure the breast in reflectance mode with a source-to-detector separation of 20 mm (Fig. 2(b)). For the measurement at each grid point, the center of the probe (i.e., the midpoint of the source and detector fiber bundle) is placed onto the point. The data acquisition time is approximately 7 minutes for a single scan.

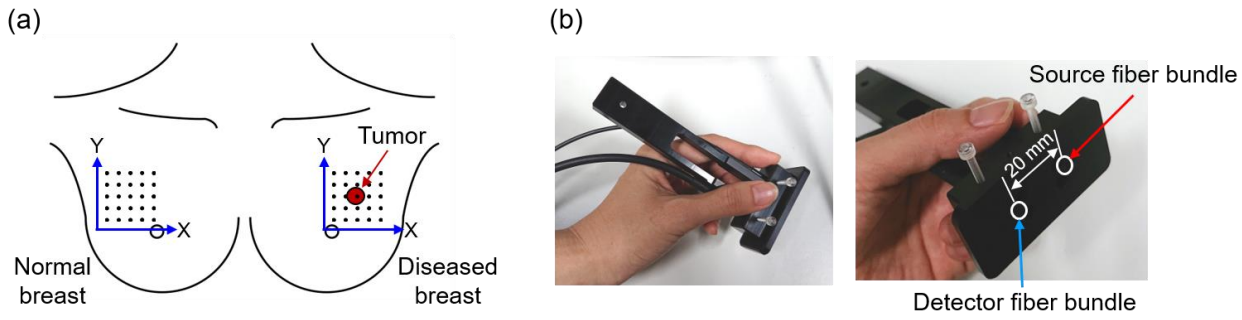

Figure 2. (a) Typical scan areas for breast measurements. The scan areas of 5 × 5 grid points with a 10-mm spacing are marked on both the diseased and contralateral normal breast. (b) Appearance of the hand-held probe. The measurements at each grid point are performed using the hand-held probe with reflectance geometry and a source-to-detector separation of 20 mm.

Image reconstruction method

Using the Rytov approximation to the photon diffusion equation (PDE), the temporal profile measured with the TD-RDOT at wavelength λ is expressed as

$$I^{\lambda}(\mu_a^{\lambda},\mu_s'^{\lambda};t)=I_{ave}^{\lambda}(\mu_{a,ave}^{\lambda},\mu_{s,ave}'^{\lambda};t)\exp\left[-\int_V W_a^{\lambda}(\mathbf{r},t)\Delta\mu_a^{\lambda}(\mathbf{r})\,d\mathbf{r}\right]\exp\left[-\int_V W_s^{\lambda}(\mathbf{r},t)\Delta\mu_s'^{\lambda}(\mathbf{r})\,d\mathbf{r}\right]. \quad (1)$$

Here, μ_a and μ_s' are the absorption and reduced scattering coefficients, and $I_{ave}^{\lambda}(\mu_{a,ave}^{\lambda},\mu_{s,ave}'^{\lambda};t)$ is the temporal profile for the average values of the optical properties ($\mu_{a,ave}^{\lambda}$ and $\mu_{s,ave}'^{\lambda}$) obtained through the TD-RDOT scan. As the TD-RDOT is capable of quantifying the optical properties at a measurement point using an analytical solution of the PDE for a semi-infinite homogeneous medium, $\mu_{a,ave}^{\lambda}$ and $\mu_{s,ave}'^{\lambda}$ of the scan area can be calculated by taking the respective averages of μ_a and μ_s' measured at all grid points. $\Delta\mu_a^{\lambda}(\mathbf{r})$ and $\Delta\mu_s'^{\lambda}(\mathbf{r})$ are the differences between the spatial distributions of the optical properties and their average values. $W_a^{\lambda}(\mathbf{r},t)$ and $W_s^{\lambda}(\mathbf{r},t)$ are weight functions that relate the optical properties inside the medium to the measured temporal profile, and are given by

$$\begin{cases} W_a(\mathbf{r},t)=\dfrac{c}{\phi_0(\mathbf{r}_s;\mathbf{r}_d,t)}\displaystyle\int_0^t G(\mathbf{r}';\mathbf{r}_d,t-t')\phi_0(\mathbf{r}_s;\mathbf{r}',t')\,dt' \\ W_s(\mathbf{r},t)=-3D_{ave}^2\dfrac{c}{\phi_0(\mathbf{r}_s;\mathbf{r}_d,t)}\displaystyle\int_0^t \nabla G(\mathbf{r}';\mathbf{r}_d,t-t')\cdot\nabla\phi_0(\mathbf{r}_s;\mathbf{r}',t')\,dt' \end{cases}, \quad (2)$$

where $\mathbf{r}_s$ and $\mathbf{r}_d$ are source and detector positions, $G(\mathbf{r};\mathbf{r}_d,t)$ is the Green's function solution of the PDE at $\mathbf{r}_d$ for a point source at $\mathbf{r}$, and $\phi_0(\mathbf{r}_s;\mathbf{r},t)$ is the solution of the PDE at $\mathbf{r}$ for a point source at $\mathbf{r}_s$. $D_{ave}=1/(3\mu_{s,ave}')$ is the average value of the diffusion coefficient, and c is the speed of light in the medium. The three-dimensional distributions of μ_a^{λ} and $\mu_s'^{\lambda}$ are restored by solving the non-linear least squares problem that minimizes the objective function defined as

$$\chi^2=\sum_{\lambda=1}^{6}\sum_{q=0}^{Q-1}\sum_{n=0}^{N-1}\frac{\left[y_q^{\lambda}(t_n)-I_q^{\lambda}(\mu_a^{\lambda},\mu_s'^{\lambda};t_n)\right]^2}{y_q^{\lambda}(t_n)}, \quad (3)$$

where $y_q^{\lambda}(t_n)$ and $I_q^{\lambda}(\mu_a^{\lambda},\mu_s'^{\lambda};t_n)$ are the measured and estimated temporal profiles for the qth grid point at discrete time t_n. A non-linear conjugate gradient algorithm is used to minimize χ^2. Images of O_2Hb, HHb, water, and lipid contents are obtained from the reconstructed distributions of μ_a^{λ}. tHb and StO_2 are calculated from O_2Hb and HHb (tHb = O_2Hb + HHb and StO_2 = 100 × O_2Hb/tHb). The reconstruction region has a width of 50 mm, length of 50 mm, and depth of 30 mm, and is discretized into 5-mm voxels. The computation time for image reconstruction of the data from a single scan is about 2.5 minutes.

RESULTS AND DISCUSSION

We conducted preliminary clinical measurements to examine the performance of the TD-RDOT system for imaging breast cancer. Measurements were made for a 42-year-old female breast cancer patient with a tumor in the upper outer quadrant of the left breast. Figure 3 shows the position of the tumor in the breast and ultrasound images of the tumor in transverse and sagittal planes. The nipple to tumor distance was 57 mm, the distance from the skin to the anterior surface of the tumor was 1.35 mm, and the tumor size was 20 × 20 × 17 mm. Figure 4 shows reconstructed three-dimensional distributions of tHb, StO_2, water, and lipid contents. The distribution in the reconstruction region is represented by seven XY slices at depth intervals of 5 mm. The reconstructed images show that the breast cancer had high tHb and water content, and low StO_2 and lipid content. The maximum tHb value in the diseased breast was 54.7 μM, which was 31.1 μM higher than the average value of 23.6 μM in the normal breast. The maximum water content value in the diseased breast was 44.3%, which was 33.8% higher than the average value of 10.5% in the normal breast. The minimum StO_2 value in the diseased breast was 73.8%, which was 3.5% lower than the average value of 77.3% in the normal breast. The minimum value for lipid content in the diseased breast was 46.9%, which was 24.7% lower than the average value of 71.6% in the normal breast. We consider that high tHb reflects vascularization caused by tumor growth and that low StO_2 implies hypoxia in the tumor. We also believe that increased cellularity of the tumor, inflammation, and edema around the tumor cause a high water content, and that the extrusion of adipose tissue by tumor growth leads to low lipid content.

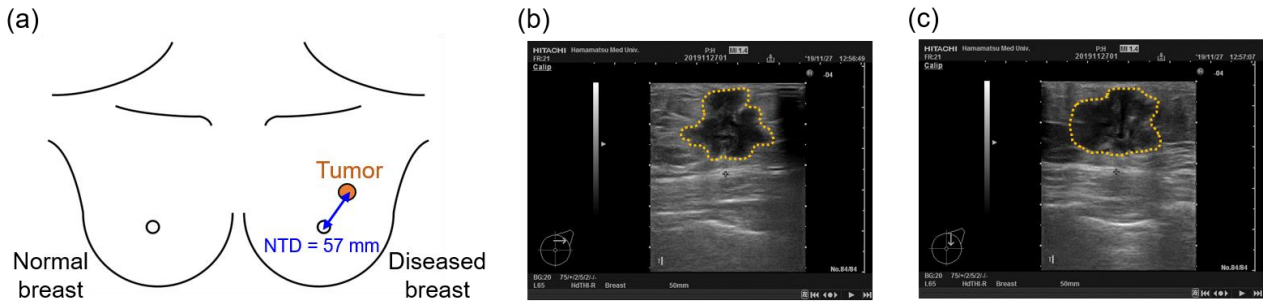

Figure 3. (a) Position of the tumor in the breast. Ultrasound images of the tumor in (b) transverse and (c) sagittal planes. Yellow dashed lines in the ultrasound images show the outline of the tumor. The tumor was situated in the upper outer quadrant of the left breast. The nipple to tumor distance (NTD) was 57 mm, the distance from the skin to the anterior surface of the tumor was 1.35 mm, and the tumor size was 20 × 20 × 17 mm.

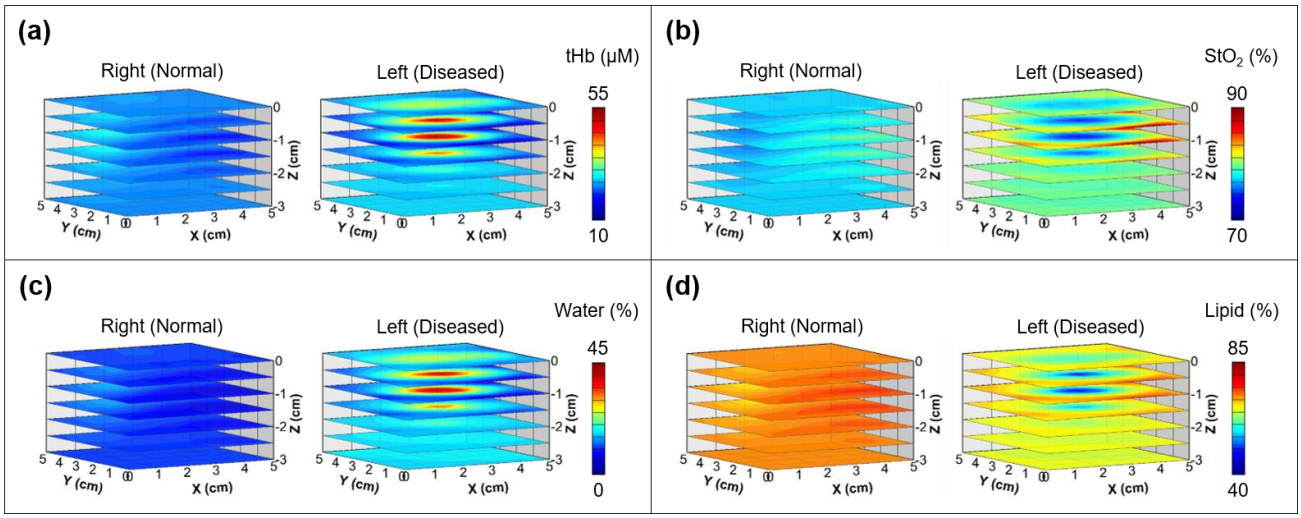

Figure 4. Reconstructed three-dimensional distributions of (a) total hemoglobin concentration (tHb), (b) tissue oxygen saturation (StO_2), (c) water content, and (d) lipid content for the breast cancer patient. A 20 × 20 × 17 mm tumor was present in the upper outer quadrant of the left breast. The reconstruction region has a width of 50 mm, length of 50 mm, and depth of 30 mm, and the parameters are represented by seven XY slices at 5-mm depth intervals.

CONCLUSION

We presented a TD-RDOT system designed to provide three-dimensional images of the tHb, StO_2, water, and lipid contents of breast cancer for the monitoring of responses to neoadjuvant chemotherapy. A scan area of 5 × 5 grid points marked on the breast surface was scanned in reflectance mode using the single-channel TD-DOS system and a hand-held probe. An iterative image reconstruction algorithm was used to generate three-dimensional images of the tissue parameters. The results of a preliminary clinical measurement demonstrate that the TD-RDOT system has the potential to provide images of various tissue parameters in breast cancer. Further studies are planned to improve localization of deeper regions and monitor the responses to breast cancer chemotherapy at the bedside.

REFERENCES

[1] Grosenick, D., Rinneberg, H., Cubeddu, R. and Taroni, P., "Review of optical breast imaging and spectroscopy," J. Biomed. Opt. 21(9), 091211 (2016).

[2] Taroni, P., Paganoni, A. M., Ieva, F., Pifferi, A., Quarto, G., Abbate, F., Cassano, E. and Cubeddu, R., "Non-invasive optical estimate of tissue composition to differentiate malignant from benign breast lesions: A pilot study," Sci. Rep. 7, 40682 (2017).

[3] Yazdi, H. S., O'Sullivan, T. D., Leproux, A., Hill, B., Durkin, A., Telep, S., Lam, J., Yazdi, S. S., Police, A. M., Carroll, R. M., Combs, F. J., Strömberg, T. Yodh, A. G., and Tromberg, B. J., "Mapping breast cancer blood flow index, composition, and metabolism in a human subject using combined diffuse optical spectroscopic imaging and diffuse correlation spectroscopy," J. Biomed. Opt. 22(4), 045003 (2017)

[4] Altoe. M. L., Marone, A., Kim, H. K., Kalinsky, K., Hershman, D. L., Hielscher, A. H. and Ha, R. S., "Diffuse optical tomography of the breast: a potential modifiable biomarker of breast cancer risk with neoadjuvant chmotherapy," Biomed. Opt. Express 10(8), 4305-4315 (2019).

[5] Tromberg, B. J., Zhang, Z, Leproux, A., O'Sullivan, T. D., Cerussi, A. E., Carpenter, P. M., Mehta, R. S., Roblyer, D., Yang, W., Paulsen, K. D., Pogue, B. W., Jiang, S., Kaufman, P. A., Yodh, A. G., Chung, S. H., Schnall, M., Snyder, B. S., Hylton, N., Boas, D. A., Carp, S. A., Isakoff, S. J. and Mankoff, D., on behalf of the ACRIN 6691 investigators, "Predicting Responses to Neoadjuvant Chemotherapy in Breast Cancer: ACRIN 6691 Trial of Diffuse Optical Spectroscopic Imaging," Cancer Res. 76, 5933-5944 (2016).

[6] Cochran, J. M., Busch, D. R., Leproux, A., Zhang, Z., O'Sullivan, T. D., Cerussi, A. E., Carpenter, P. M., Mehta R. S., Roblyer, D., Yang, W., Paulsen, K. D., Pogue, B., Jiang, S., Kaufman, P. A., Chung, S. H., Schnall, M., Snyder, B. S., Hylton, N., Carp, S. A., Isakoff, S. J., Mankoff, D., Tromberg, B. J. and Yodh, A. G., "Tissue oxygen saturation predicts response to breast cancer neoadjuvant chemotherapy within 10 days of treatment," J. Biomed. Opt. 24(2), 021202 (2019).

[7] Tank, A., Peterson, H. M., Pera, V., Tabassum, S., Leproux, A., O'Sullivan, T., Jones, E., Cabral, H., Ko, N., Mehta, R. S., Tromberg, B. J. and Roblyer, D., "Diffuse optical spectroscopic imaging reveals distinct early breast tumor hemodynamic responses to metronomic and maximum tolerated dose regimens," Breast Cancer Res. 22, 29 (2020).

[8] Zhang, M., Shihab Uddin, K. M., Li, S. and Zhu, Q., "Target depth-regularized reconstruction in diffuse optical tomography using ultrasound segmentation as prior information," Biomed. Opt. Express 11(6), 3331-3345, (2020)

[9] Zouaoui, J., Sieno, L. D., Herve, L, Pifferi, A., Farina, A., Mora. A. D., Derouard, J. and Dinten, J., "Chromophore decomposition in multispectral time-resolved diffuse optical tomography," Biomed. Opt. Express 8(10), 4772-4787, (2017).

[10] Yoshimoto, K., Ohmae, E., Yamashita, D., Suzuki, H., Homma, S., Mimura, T., Wada, H., Suzuki, T., Yoshizawa, N., Nasu, H, Ogura, H., Sakahara, H., Yamashita, Y. and Ueda, Y., "Development of time-resolved reflectance diffuse optical tomography for breast cancer monitoring," Proc. SPIE 10059, 100590M, (2017).

[11] Ohmae, E., Yoshizawa, N., Yoshimoto, K., Hayashi, M., Wada, H., Mimura, T., Suzuki, H., Homma, S., Suzuki, N., Ogura, H., Nasu, H., Sakahara, H., Yamashita, Y. and Ueda, Y., "Stable tissue-simulating phantoms with various water and lipid contents for diffuse optical spectroscopy," Biomed. Opt. Express 9(11), 5792-5807 (2018).

[12] Suzuki, H., Ohmae, E., Yoshimoto, K., Wada, H., Homma, S., Suzuki, N., Mimura, T., Yamashita, Y. and Ueda, Y., “Water and lipid contents measured at various parts of the human body with a six-wavelength time-resolved spectroscopy system,” Proc. SPIE 10874, 108740A, (2019).
[13] Ohmae, E., Yoshizawa, N., Yoshimoto, K., Hayashi, M., Wada, H., Mimura, T., Asano, Y., Ogura, H., Yamashita, Y., Sakahara, H. and Ueda, Y., “Comparison of Lipid and Water Contents by Time-domain Diffuse Optical Spectroscopy and Dual-energy Computed Tomography in Breast Cancer Patients,” Appl. Sci. 9(7), 1482 (2019).